Supporting Information

Selenium Embedded in MOFs-derived N-doped Microporous Carbon Polyhedrons as a High Performance Cathode for Sodium-Selenium Batteries

Siqi Li,[1] Hai Yang,[1] Rui Xu,[1] Yu Jiang,[1] Yue Gong,[3] Lin Gu[3], Yan Yu*[1,2]

[1]Department of Materials Science and Engineering, University of Science and Technology of China, CAS Key Laboratory of Materials for Energy Conversion, Hefei, 230026, Anhui, P. R. China
[2]Institute of Advanced Electrochemical Energy, Xi'an University of Technology, Xi'an 710048, China
E-mail: yanyumse@ustc.edu.cn
[3]Beijing National Laboratory for Condensed Matter Physics
The Institute of Physics, Chinese Academy of Sciences, Beijing 100190, China

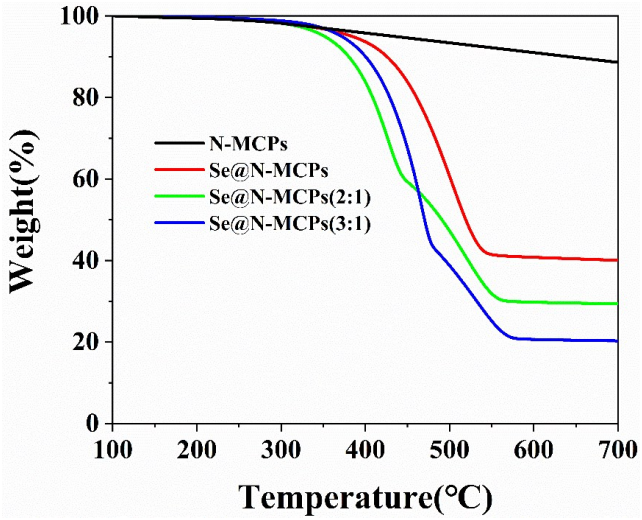

Fig.S1 TG profiles of the obtained composites with various ratios of Se versus N-MCPs. the content of Se distributed in the porous carbon polyhedrons was determined to be 48.55%, 59.23%, and 68.31%, respectively.

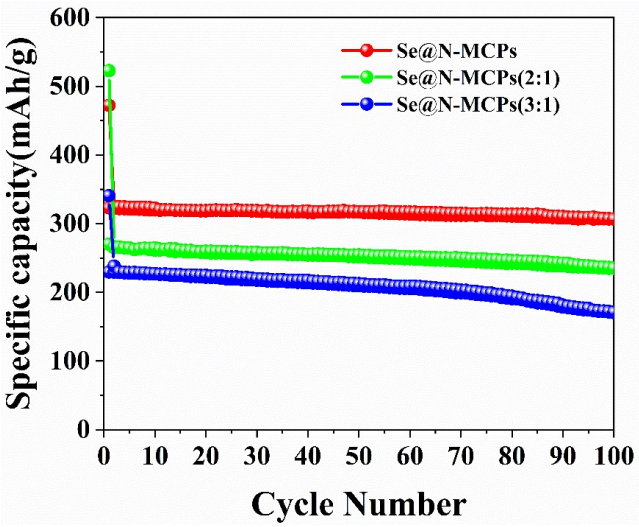

Fig. S2 Cyclic performances of the composites with various ratios of Se versus N-MCPs at a current density of 0.1 A g^{-1}(the specific capacity is based on the composite).

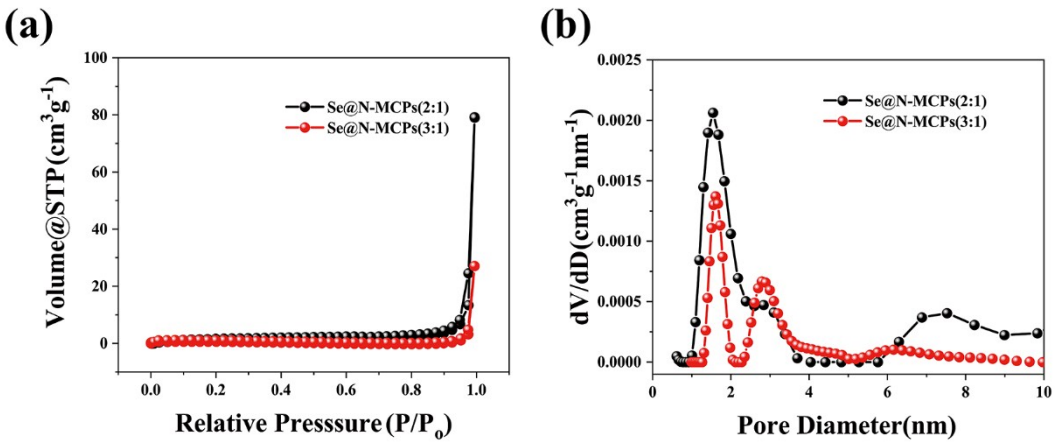

Fig.S3 a) N_2 adsorption desorption isothermal curves and b) the corresponding pore-size distribution curves of Se@N-MCPs (2:1) and Se@N-MCPs (3:1).

Table S1 Comparison of BET performance among N-MCPs and Se@N-MCPs at various content of Se.

Samples	BET Specific Surface Area (m^2g^{-1})	Pore Volume (cm^3g^{-1})	Pore size (nm)
N-MCPs	980.992	0.478	0.548
Se@N-MCPs	16.175	0.037	1.667
Se@N-MCPs(2:1)	3.268	0.022	1.543
Se@N-MCPs(3:1)	2.528	0.003	1.610

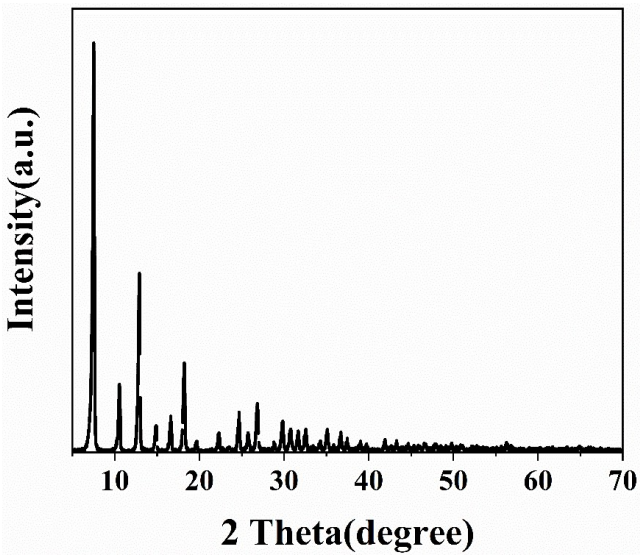

Fig. S4 XRD pattern of ZIF-8 nanocrystals.

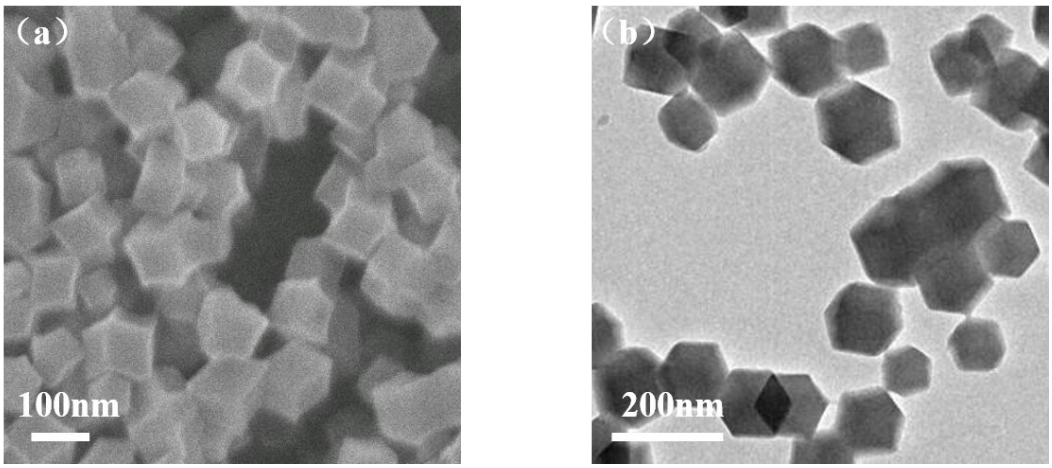

Fig.S5 a) SEM, b) TEM images of ZIF-8 nanocrystals.

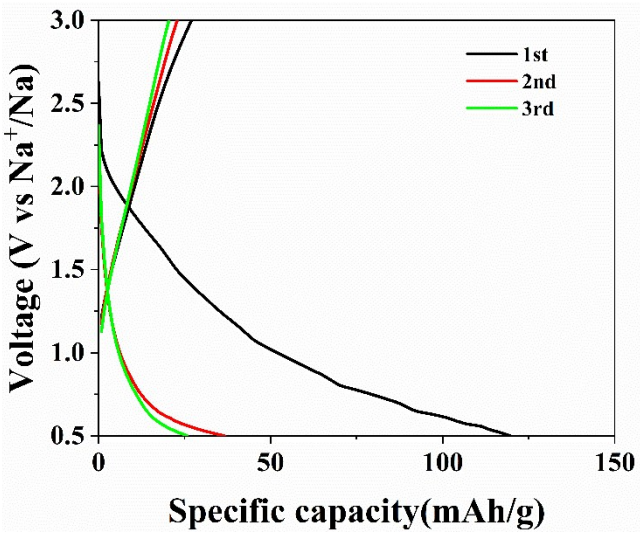

Fig.S6 Galvanostatic charge/discharge profiles of the N-MCPs at a current density of 0.1 A g^{-1}

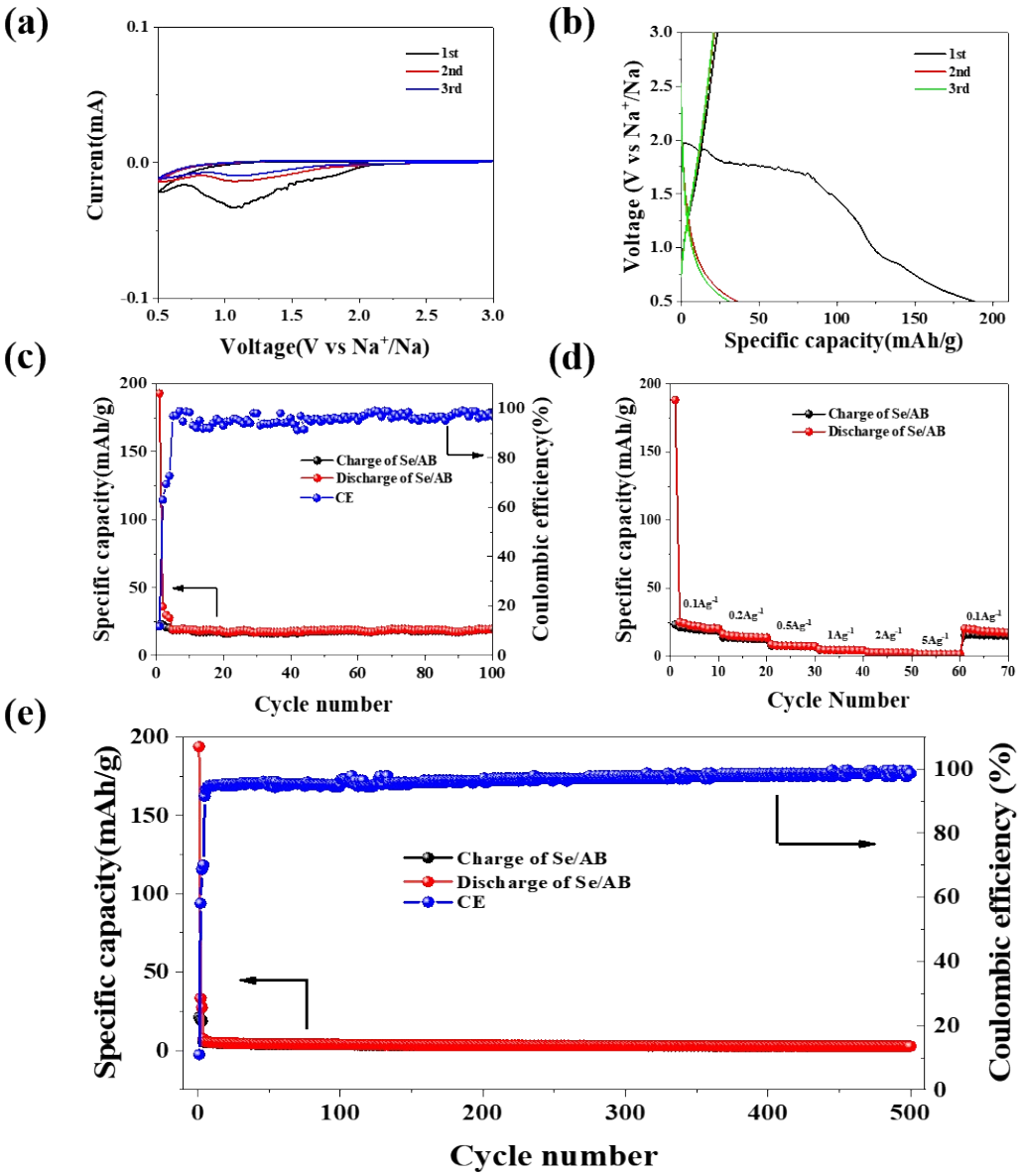

Fig. S7 a) Cyclic voltammograms of the Se/AB electrodes at a scan rate of 0.1 mV s^{-1} in the voltage window from 0.5 V to 3 V versus Na^+/Na. (b) Galvanostatic charge/discharge profiles of the Se/AB electrodes at a current density of 0.1 A g^{-1} between 0.5 V and 3 V versus Na^+/Na. (c) Cyclic performance of the Se/AB electrodes at a current density of 0.1 A g^{-1} . (d) Rate capability of the Se/AB electrodes at various current densities. (e) A long-term cyclic performance of the Se/AB electrodes at a current density of 1 A g^{-1}.

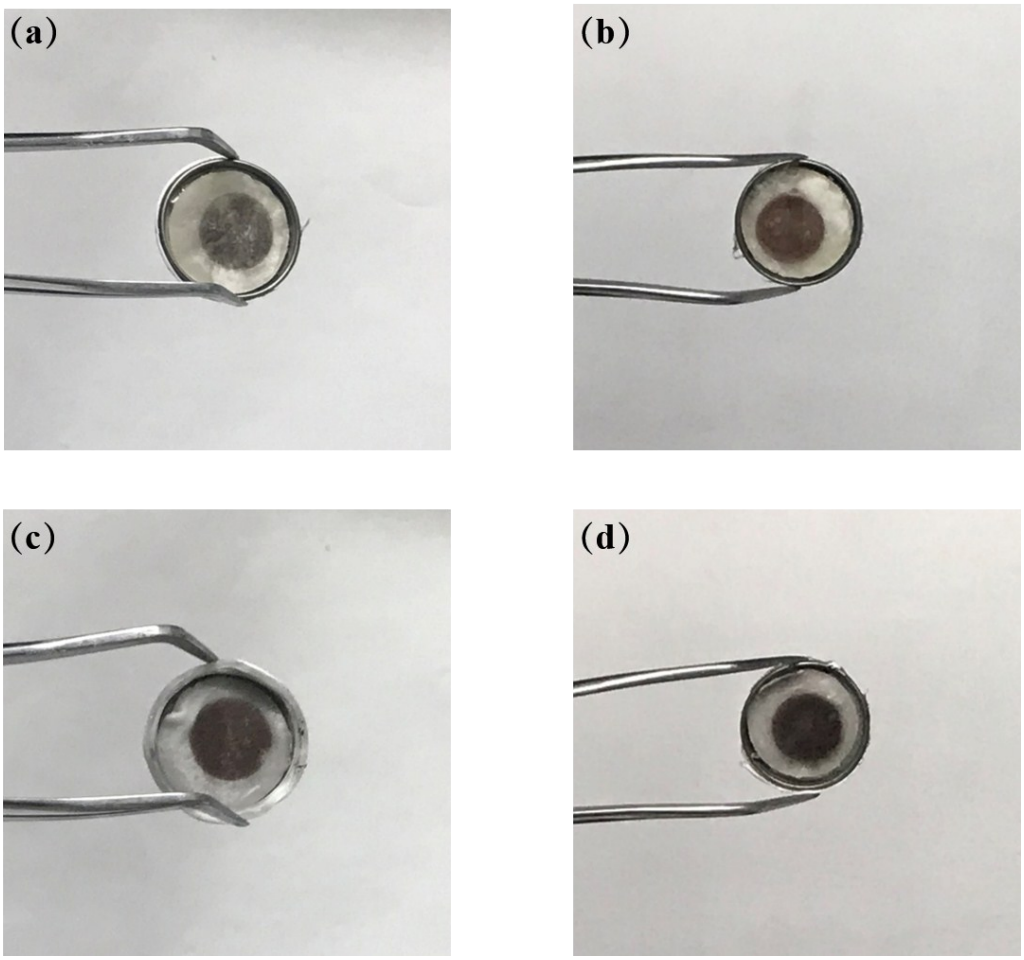

Figure S8. The color change of electrolyte in the (a) Se@N-MCPs, (b) Se@N-MCPs (2:1), (c) Se@N-MCPs (3:1), (d) Se/AB cells after cycling.

Table S2. The long cycling performance comparison for the published Se-based cathodes for Na–Se batteries.

Materials	Current density	Reversible	References	Se

	(A g^{-1})	capacity (mAh g^{-1})		loading(wt%)
Se/C	0.16875	340 after 380 cycles	[1]	30
CPAN/Se	0.2025	410 after 300 cycles	[2]	36
Se@CNFs-CNT	0.5	410 after 240 cycles	[3]	35
Se@PCNFs	0.05	520 after 80 cycles	[4]	52.3
Se/(CNT@MPC)	0.675	440 after 100 cycles	[5]	50.2
SC@Se-Al2O3	0.5	503 after 1000 cycles	[6]	67
NHCS/Se	0.3375	330 after 50 cycles	[7]	52
Se/NPCPs	1.35	161.4 after 1000 cycles	[8]	48.5
Se-CCN	0.135	514 after 500 cycles	[9]	53
Se-NCMC	0.135	475 after 300 cycles	[10]	70
CNF/Se	0.3375	478 after 200 cycles	[11]	72.1
Se/MCNFs	0.5	430 after 200 cycles	[12]	48
Se@N-MCPs	1	460 after 500 cycles	This work	48.55

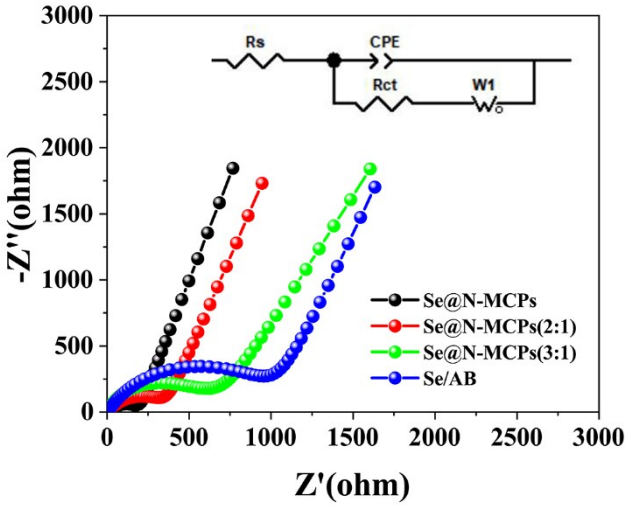

Fig.S9. The Nyquist plots of the Se@N-MCPs, Se@N-MCPs (2:1), Se@N-MCPs (3:1) and Se/AB electrodes after three cycles with equivalent circuit inset. The Rct of each electrode is 195 Ω, 278 Ω, 484 Ω, 964 Ω, respectively.

References

1 C. Luo, Y. Xu, Y. Zhu, Y. Liu, S. Zheng, Y. Liu, A. Langrock, C. Wang, *ACS Nano*, 72013, 7, 8003-8010.

2 H. Wang, S. Li, Z. Chen, H.K. Liu, Z. Guo, *RSC Adv.*, 2014, 4, 61673-61678.

3 L. Zeng, X. Wei, J. Wang, Y. Jiang, W. Li, Y. Yu, *J. Power Sources*, 2015, 281, 461-469.

4 L. Zeng, W. Zeng, Y. Jiang, X. Wei, W. Li, C. Yang, Y. Zhu, Y. Yu, *Adv.Energy Mater.*, 2015, 5, 1401377.

5 S. Xin, L. Yu, Y. You, H.P. Cong, Y.X. Yin, X.L. Du, Y.G. Guo, S.H. Yu, Y. Cui, J.B. Goodenough, *Nano Lett.*, 2016, 16, 4560-4568.

6 D. Ma, Y. Li, J. Yang, H. Mi, S. Luo, L. Deng, C. Yan, P. Zhang, Z. Lin, X. Ren, J. Li, H. Zhang, *Nano Energy*, 2018, 43, 317-325.

7 B. Kalimuthu, K. Nallathamby, *ACS Appl. Mater. Interfaces*, 2017, 9, 26756-26770.

8 Q. Xu, T. Liu, Y. Li, L. Hu, C. Dai, Y. Zhang, Y. Li, D. Liu, M. Xu, *ACS Appl. Mater. Interfaces*, 2017, 9, 41339-41346.

9 J. Ding, H. Zhou, H. Zhang, T. Stephenson, Z. Li, D. Karpuzov, D. Mitlin, *Energy Environ. Sci*, 2017, 10, 153-165.

10 J. Ding, H. Zhou, H. Zhang, L. Tong, D. Mitlin, *Adv. Energy Mater.*, 2017, 8, 1701918.

11 H. Wang, Y. Jiang, A. Manthiram, *Adv. Energy Mater.*, 2018, 8, 1701953.

12 B. Yuan, X. Sun, L. Zeng, Y. Yu, Q. Wang, *Small*, 2018, 14, 1703252.